ELSEVIER

Ceramics International 28 (2002) 439–445

CERAMICS INTERNATIONAL

www.elsevier.com/locate/ceramint

Effect of powder, chemistry and morphology on the dielectric properties of liquid-phase-sintered alumina

Amiya P. Goswami[a,*], Sukumar Roy[a], Gopes C. Das[b]

[a]*Ceramic Technological Institute, Bharat Heavy Electricals Limited, Bangalore 560 012, India*
[b]*Department of Metallurgical Engineering, Jadavpur University, Calcutta 700 032, India*

Received 23 November 2000; received in revised form 2 August 2001; accepted 9 October 2001

Abstract

Dielectric properties of liquid-phase-sintered alumina (LPS) ceramics prepared using commercial powders of different particle size distribution and impurities (Na_2O) content were studied. So far as the particle size distribution of the commercial powder is concerned, LPS ceramics, those derived from powders of both medium (3.1–8.4 μm) and coarse (70–100 μm) grades, showed similar dielectric loss, whereas it was higher in the case of LPS derived from the reactive powders (<1 μm). While considering the impurity levels of the powders, higher Na_2O content (0.57 wt.%) in the powder showed significantly higher dielectric loss compared to that of the lower Na_2O content (<0.2 wt.%). Furthermore, the MgO/(CaO + BaO + KNaO) ratio in the chemical composition of the LPS within the range of 0.4–1.8 was found to influence the dielectric properties in the frequency range of 10^2–10^7 Hz. The dielectric loss in the frequency band of 10^2–10^3 Hz was found to be higher in the case of the LPS with a MgO/(CaO + BaO + KNaO) ratio of 1.6. Besides the starting powder and the chemical composition, the orientation of alumina platelets arising out of fabrication route (e.g. tape casting) was also found to have a profound influence on the dielectric properties. A higher loss was observed in the tape cast specimen.

Keywords: A. Tape casting; B. Impurities; C. Dielectric properties; D. Alumina

1. Introduction

Ceramic materials have been broadly classified into insulators and semiconductors based on dielectric constant [1]. Generally, materials with dielectric constant less than 12 are classed as insulators and dielectric constant above 12 is capacitors [1]. Alumina is a low loss dielectric material. The dielectric constant of alumina places it well within the insulating range with a value of 8.8 at 1 MHz [1]. The loss tangent of materials at lower frequencies depends on the ease of migration of ions under the influence of the a.c. field. The loss factor of alumina is about 0.001, that is again low enough to satisfy conditions for insulating applications [1]. Alumina is a dominant ceramic material not only because of its superior mechanical, thermal, and chemical properties, but also because of outstanding electrical properties. The electrical properties make it adaptable for use in many applications ranging from electronic substrates to spark plug insulators to MHD power generators.

Impurities at the grain boundary are known to influence the electrical characteristics [1–13]. Concerning the purity aspects of the raw materials—alkali, iron and titania impurities are reported to be the most influential on the electrical properties [1]. Second-phase distribution, alkali content and working temperature alter the dielectric behavior in alumina ceramics. In glasses, for example, Na_2O, CaO, and Al_2O_3 are known to produce a decrease in resistivity [3,4]. Na_2O is the chief impurity in commercial alumina powders, that mostly lies in the level of 0.1–0.4 wt.% and in some as high as 0.7 wt.%. The particle sizes, however, vary widely starting from submicron to 100 μm depending on the commercial sources. A vast number of alumina ceramics are produced by reactive liquid phase sintering using alkaline earth silicates as sintering additives (LPS) and thus a significant amount of second phases remains in the grain boundary as glass. Alumina ceramics with crystalline α-alumina separated by a vitreous silicate boundary layer may have properties between those of single crystal alumina

* Corresponding author. Tel.: +91-33-672-3535; fax: +91-33-672-2705.
E-mail address: jsir@vsnl.cal.net.in (A.P. Goswami).

0272-8842/02/$22.00
PII: S0272-8842(01)00116-X

and glass [1]. Anisotropy in dielectric properties may also need to be taken into account if the permittivity of a single crystal of any of the major phases is anisotropic. For example, there is a 20% difference in permittivity between a- and c-axis directions in sapphire [2]. A fine-grained alumina ceramic in which the individual crystals have a non-random orientation, as in an extruded or tape cast product, may also be anisotropic [14,15].

In our previous report, it was shown that the MgO/(CaO + BaO + KNaO) ratio and SiO_2 content in the chemical composition of the LPS play a dominant role on the microstructure (grain size, grain shape and intergranular phases) resulting in significant differences of the mechanical and the tribological properties [16–19]. The aforesaid ratio was investigated in the range of 0.4–2.0 in 91–94 wt.% Al_2O_3 containing LPS materials derived from medium (3.1–8.4 μm) and coarse (70–100 μm) sized powders. LPS of lower ratio had more elongated grains while that of the higher ratio had more equiaxed grains.

The objective of the present study is to investigate the role of particle size and impurity level (Na_2O) in the starting powder on the dielectric properties. The role of MgO/(CaO + BaO + KNaO) ratio in the chemical composition of the LPS on the electrical properties shall also be investigated. Additionally, the effect of particle orientation due to the fabrication route shall be examined.

2. Experimental

All the starting powders are from commercial sources. On the basis of the particle size, the alumina powders of the lowest size range (<1.0 μm) are termed here as reactive or those with higher size range as non-reactive as similarly designated elsewhere [20]. Alumina powders (both non-reactive and reactive varieties) with different particle size distribution and purity were selected from different origins. The non-reactive powders that possess a particle size distribution in the range of 3.1–8.4 μm are termed as "medium" and those in the range of 70–100 μm as "coarse". In the medium variety, 'I' grade had Na_2O content (wt.%) of 0.19 and 0.30. 'M' and 'S' belong to coarse variety and had Na_2O content of 0.57 and 0.29 respectively. Likewise, the reactive powders were comprised of two grades, namely 'R' and 'A16SG' (specific surface area of about 10 m^2/gm), both with Na_2O content of 0.1 wt.%. The chemical and physical properties of these powders have been reported elsewhere [16].

Different LPS ceramics were prepared using the above powders and different sintering additives. The proportion of the constituents' e.g. Na_2O, CaO, MgO, BaO, SiO_2, F_2O_3 and TiO_2 in the chemical composition of the LPS was also varied in each class.

Alumina powder along with the required amounts of sintering aids were thoroughly mixed in the appropriate ratio and ball-milled using alumina bowl and balls for 16 h in deionsed water medium. The mixed composition was then oven dried, fabricated in the form of pellets by uniaxial pressing and fired in air following the same procedure as mentioned earlier [16]. One of the compositions was also fabricated by tape casting using the doctor blade technique [14,15]. Chemical composition, grain size and its shape, intergranular phases, volume percentage of glass and pore in these sintered LPS materials were presented in our previous reports [16–19].

The grain size and shape of the LPS alumina ceramics are dependent on the MgO/(CaO + BaO + KNaO) ratio in the chemical composition [16]. Depending on the ratio, the materials have been further classified. In 91–94 wt.% LPS, MgO/(CaO + BaO + KNaO) ratio of <1.0, 1.0–1.5 and 1.5–2.0 are represented by 'A', 'B' and 'C' respectively [16]. 95–97 wt.% LPS has been represented by 'H' irrespective of the ratio. For identification, the grade of the powder used has been mentioned in the suffix of the material code. Dense LPS ceramics with open porosity less than 0.1% has been used for further study. Specimens of $A1_I$, $A6_M$ $A7_R$, $A8_R$, $C1_I$, $C2_Si$, $C4_I$ and $H3_{A16}$ have been prepared by uniaxial pressing and $C2_Si$ has also been prepared by tape casting [19].

2.1. Volume resistivity

Specimens for these tests were thin discs of 12–14 mm diameter with thickness of nearly 1 mm. Uniform thickness (±0.05 mm) and smooth surface finish was maintained by grinding and lapping with SiC grits and diamond paste successively. After cleaning in an ultrasonic bath, specimens were oven dried at 110 °C for 24 h and then cooled in a desiccator. Both faces of the specimen were gold coated by sputtering. In addition, layers of silver paste were applied repeatedly until the surface resistance was less than 1 Ω. A digital LCR meter (Sortester made by Aplab, India) measured both the surface resistance and the volume resistance. The layer of conducting metal at the outer face of the specimen was carefully removed with the help of a fine SiC (No. 800) paper and acetone so as to avoid direct contact between the faces. If the resistance within the plane of the specimen was low and a value of the order of 10^6 Ω between the opposite faces was observed, the specimen was then accepted for further testing.

2.2. Leakage current in d.c. applied voltage

Leakage current was measured by a 'break down tester' (model RM 215G of BPL India) at 10 kV d.c. applied voltage. Specimens of diameter 74–77 mm and thickness 0.9–1.2 mm were prepared by uniaxial pressing. The specimens were cleaned in an ultrasound water bath and oven dried at 110 °C for 24 h and then allowed to

cool down in a desiccator. A conducting silver paint (resin bond) of ~5 mm diameter was applied on the same spot of the opposite faces using a zig. The resin was heated to set in an oven at 110 °C for a period of 2 h. A set of two such spots in each face of the specimen was marked at a distance of 25 mm. Opposite spots of the specimen with a conducting layer was tightly held in between the pointed electrodes for the purpose of applying the voltage. The applied voltage was gradually increased in steps of 1 kV and held for duration of 1 min. Both the leakage current and the applied voltage at the time of discharge were recorded. After the test, the specimens were subjected to a 'die penetration test' for the porosity check. The test was conducted at a pressure of 25 MPa and for duration of 8 h. The penetration of the die-solution into the subsurface area was visually examined after breaking the specimen. The discharge path was also carefully observed later on under an optical microscope (×50) for identification of defects.

2.3. Dissipation factor, relative dielectric constant and loss factor at different frequency

In order to determine the effect of MgO/(CaO + BaO + KNaO) ratio on the capacitance (Cp) and the dissipation factor (d.f.), tests were conducted on the two non-reactive 91–94 wt.% LPS of low and high MgO/(CaO + BaO + KNaO) ratio. $A1_I$ (ratio of 0.41) and $C1_I$ (ratio of 1.57) were the two materials. An impedance analyzer (Hewlett Packard, model 4194 A) measured the *Cp* and *d.f.* in the frequency range starting from 100 Hz to 40 MHz. The digitized output was collected through a computer and the relative dielectric constant (k') was calculated from the measured *Cp* using the following formula.

$$k' = Cp.d/(\varepsilon_o.A) \quad (1)$$

where, d is the distance between the parallel plate of capacitor, A is the contact area and $\varepsilon_o = 8.85$ picofarad/meter.

The loss factor is obtained by multiplication of k' and *d.f.* The loss factor (%), *d.f.* (%) and k' were then plotted against frequency.

In the case of other LPS ceramics, *Cp* and *d.f.* were measured at a frequency of 1 MHz only. Four readings were taken for each of the specimens and the average was calculated. Tests were conducted using the same specimens for volume resistivity test.

2.4. Voltage dependence of dissipation factor in power frequency

The test set up has been described in ASTM D150-92 [21]. The test was conducted using a transformer of 30 kV capacity transformer (KEC, India) that supplies power at 50 Hz frequency and applied voltage can be increased up to 4 kV. Both the capacitance and the dissipation factor were noted down from the digital display. The test was conducted on a LPS ceramics, $A6_M$, derived from a high Na_2O (0.57 wt.%) alumina powder. Specimens in the shape of disk with a diameter of 75 mm and thickness of 4.30 mm were fabricated by uniaxial powder compaction. The surface of the disk was ground to minimise the variation in thickness to less than 0.05 mm. One of the faces was completely coated with a conducting material (silver) while the opposite face was not entirely coated but an annular area in between the diameters 50 and 60 mm was left uncoated to place a guard electrode so as to avoid the 'effect due to gas conduction'.

3. Results and discussion

3.1. Micrographs of starting powder and sintered LPS

Fig. 1 (a–c) shows the differences in the morphology of different starting powders e.g. coarse, medium and reactive. More details of these powders can be seen from our previous report [16]. The large agglomerates of coarse powder (Fig. 1a) were broken into tiny platelets of 2–10 μm during milling and mixing process.

LPS derived from coarse and medium powders (91–94 wt.%) had different grain size and shape depending on the MgO/(CaO + BaO + KNaO) ratio. As for example, the grains were more elongated in the case of $A1_I$ whereas that of the $C1_I$ were more equiaxed. On the other hand, LPS of reactive powders had equiaxed grains irrespective of the MgO/(CaO + BaO + KNaO) ratio. Fig. 2 shows the grain size, grain shape and distribution of voids typically, in a reactive 95–97 wt.% LPS ceramic. Micrographs of different LPS materials have been presented in our previous reports [16–19].

3.2. Volume resistivity

Table 1 shows that the volume resistivity for the present LPS ceramics is lower than purer alumina (~10^{12} Ω.m) and the differences among the different LPS compositions are not wide i.e. well within an order of magnitude. Interestingly, although the Na_2O content in the chemical composition of $A6_M$ is nearly double to that of $B6_I$ (0.45 and 0.21%, respectively), there is no significant change in resistivity. The microstructures of $A6_M$ and $B6_I$ are similar [16,19]. When one alkali oxide is progressively substituted for another, it has been observed that the resistivity does not vary linearly with the fraction-substituted [7]. Rather, it goes through a pronounced maximum, often but not always in the range of composition in which the two alkalis are present in nearly equimolar amounts. Conductivity increases with

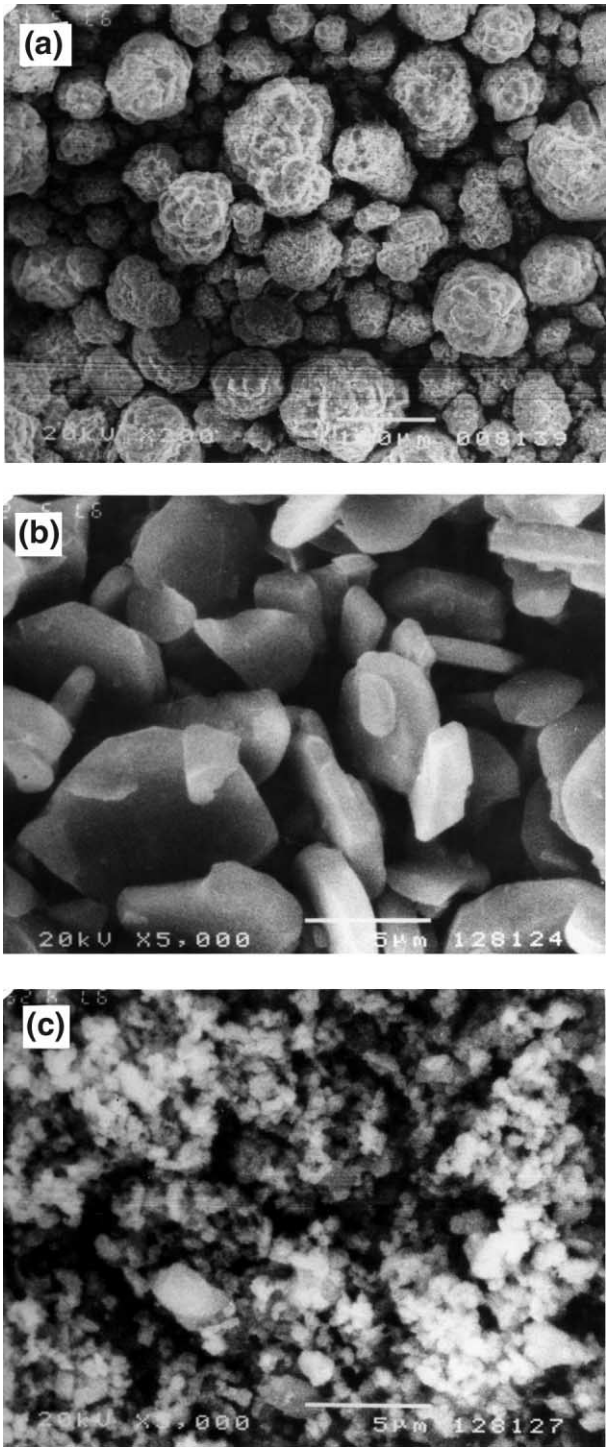

Fig. 1. Scanning electron micrographs of (a) coarse ['M' grade], (b) medium ['I' grade] and (c) thermally reactive ['R' grade] powders.

Na ion concentration but decreases when SiO_2 is replaced by modifying ion CaO, MgO, BaO or PbO and CaO [8]. Thus the 'mixed alkali effect' which appears in mechanical and dielectric relaxation as well as d.c. conductivity is associated with an interaction between ions of different types of glass [7]. Although Na_2O content is high in $A6_M$, hardly any difference in resistivity is revealed possibly due to the mixed alkali effect. Resistivites have also been observed (Table 1) to be similar in the case of the LPS materials ($A7_R$ and $H3_{A16}$) derived from reactive powders where Na_2O content is also less than 0.1% [16].

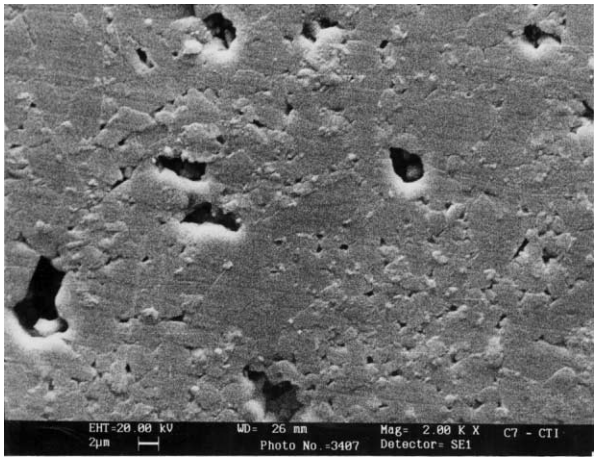

Fig. 2. Thermally etched micrograph of liquid-phase-sintered alumina ceramics ($H3_{A16}$) showing grain size, grain shape and void.

Table 1
Volume resistivity of 91–97 wt.% LPS alumina ceramics derived from powders of different purity and particle size

Material code	Resistivity Ω.m, $\times 10^8$
$A6_M$	6.45
$A7_R$	5.49
$B6_I$	8.04
$C1_I$	5.95
$C2_S$	11.81
$C2_S$[a]	11.50
$H3_{A16}$	5.24

[a] Tape cast.

3.3. Leakage current

Electrical conduction in glasses is mainly attributed to the migration of mobile ions such as Li^+, Na^+, K^+, OH^-, and H^+ under the influence of an applied d.c. field. Conduction can be ionic or electronic depending upon composition, structure and defect state. In purely crystalline materials, mobility of ions is determined by the concentration of defects, such as vacancies and impurities, in solution and at grain boundaries [2]. The strong atomic bonding in many pure oxides permits very little migration, and losses are correspondingly low. However, in glasses, especially those with alkali metals, Na and K, movement is relatively easy and losses are higher. Since the vast majority of ceramics are not of high purity, they contain glassy phases, which even in smaller amounts at grain boundaries can lead to a significant loss.

Table 2 shows that the leakage current is high due to the open porosity in the case of $A6_M$ and $C1_I$. The microscopic examination of the discharge path also showed presence of the local impurity in $C1_I$. However, the leakage current is seen to be higher in the case of $A8_R$ even though it is non-porous. The LPS materials, $A8_R$ and $A1_I$, have similar chemical composition but prepared with different powders. $A8_R$ is derived from reactive powder whereas $A1_I$ is derived from non-reactive powder. It was shown that a higher amount of alumina remains dissolved in the grain boundary glass in the case of $A8_R$ compared to $A1_I$ [18]. Alumina can enter into the glass structure either as 'AlO_4-network' former or can remain in the 'SiO_4-network' as a modifier [7]. As a network former, it is expected to stabilize the glass structure whereas as a modifier its role can possibly be different. In the present materials, the structure of grain boundary glass has not been investigated. However, a previous author has reported that the resistance of the glass decreased when alumina dissolved into the glass [3]. Present results also show that a higher amount of alumina dissolved into the glass has resulted in a higher leakage current.

3.4. Role of impurities on dielectric loss

The energy loss is proportional to frequency, so also the dissipation factors. Fig. 3 shows a comparison of the relative dielectric constant (k'), *d.f.* and loss measured at the frequency range of 100 Hz to 40 MHz for $C1_I$ and $A1_I$. In the frequency range of 10^2–10^4 Hz, the *d.f.* is normally high due to ion jump relaxation. At frequencies greater than 10^{10} Hz, *d.f.* is again high because of ion vibration and deformation [7]. However, measurement of d.f. at a frequency higher than 10^8 is not recommended in the instrument used. In the frequency range of 10^2–10^3 Hz, the material ($C1_I$) with a high MgO/(CaO + BaO + KNaO) ratio has a higher dielectric loss than that of the material ($A1_I$) with low MgO/(CaO + BaO + KNaO) ratio. Molla et al. [11] also observed similarly that a higher concentration of MgO increases loss at 10^3 Hz at room temperature. The k', however, did not show significant differences within the frequency range of 10^3–10^{10} Hz in his study. In the frequency range of 10^4–10^7 Hz, dielectric losses in these two materials are almost the same while k' is higher in $A1_I$. The bulk density and open porosity in these two materials are comparable (3.579 g/cc and 0.058% in $C1_I$, and 3.552 and 0.076% in $A1_I$). Further, it may be noted that

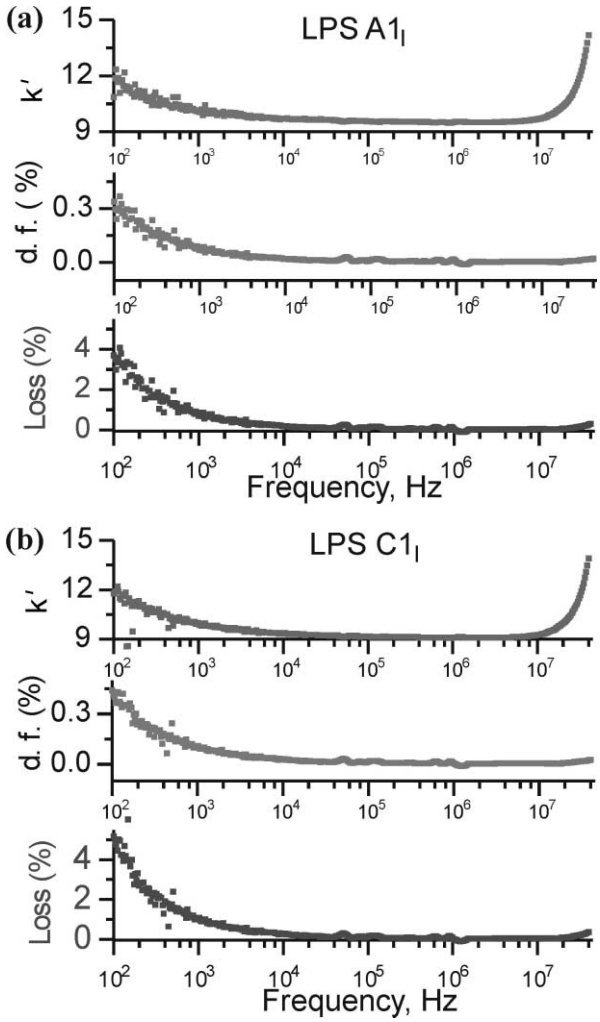

Fig. 3. Frequency dependence of dielectric constant, dissipation factor and dielectric loss in 91–94 wt.% LPS alumina with different levels of MgO/(CaO + BaO + KNaO) ratio; (a) low ratio, $A1_I$, and (b) high ratio, $C1_I$.

Table 2
Leakage current under d.c. applied voltage

Sample code	Thickness (mm)	Current and discharge voltage				Die-penetration test result
		Test I μamp	(kV)	Test II μamp	(kV)	
$A1_I$	1.18	Nil		Nil		Non-porous
$A6_M$	1.13	100	5	Nil		Porous
$B7_I$	1.83	Nil		Nil		Non-porous
$C1_I$	1.05	Nil		60	5	Porous
$C4_I$	1.17	Nil		Nil		Non-porous
$A7_R$	2.22	Nil		Nil		Non-porous
$A8_R$	0.93	80	4.5	100	3	Non-porous

Table 3
Dielectric constant, dissipation factor and loss factor for different liquid-phase-sintered aluminas

Material code		Dielectric constant	Dissipation factor (%)	Loss factor (%)	Bulk density (g/cc)	Open pore (%)
$A6_M$	Average	10.30	0.17	1.79	3.679	0.067
	σ[b]	0.025	0.023	0.240		
$A7_R$	Average	10.35	0.08	0.79	3.738	Nil
	σ	0.036	0.006	0.058		
$A8_R$	Average	12.15	0.21	2.52	3.620	Nil
	σ	0.513	0.021	0.304		
$C2_S$i	Average	9.63	0.06	0.54	3.510	0.079
	σ	0.003	0.012	0.111		
$C2_S$i[a]	Average	10.01	0.20	2.00	3.569	0.007
	σ	0.020	0.003	0.004		
$C4_I$	Average	10.29	0.04	0.42	3.472	0.088
	σ	0.167	0.002	0.213		
$H3_{A16}$	Average	10.19	0.09	0.95	3.728	Nil
	σ	0.035	0.006	0.065		

[a] Tape cast.
[b] σ, Standard deviation.

both these two materials were prepared with the same starting powder.

Table 3 shows the k', *d.f.* (%) and loss (%) measured at 1 MHz frequency. $C4_I$ with Na_2O content of 0.19 wt.% shows the lowest *d.f.* and loss. Further both the *d.f.* and the loss of $C2_s$i are comparable to $C4_I$, but the LPS with a high Na_2O content, i.e. $A6_M$, shows a steep rise in dielectric loss (Fig. 4). In the case of the LPS ceramics derived from reactive powders, the loss is found to be relatively higher (Table 3). Considering all the LPS ceramics, the highest loss is seen in $A8_R$ where the d.c. leakage current was also seen to be higher (Table 2). As already discussed a higher amount of dissolved alumina into the grain boundary glass can be a possible reason. It is thus obvious that LPS ceramics of reactive powders although produce superior mechanical properties as well as higher wear resistance, does not indicate any improvement in the electrical properties compared to that of the medium and coarse powders.

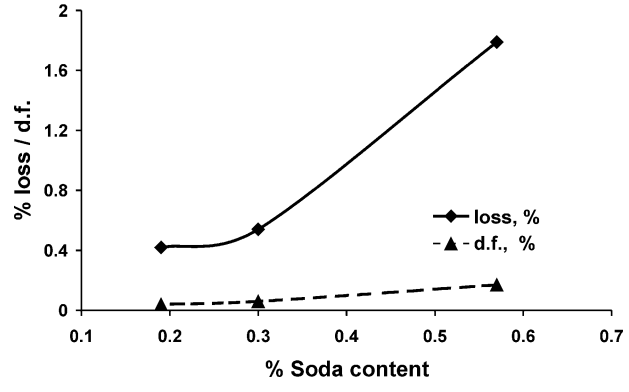

Fig. 4. Showing the effect of Na_2O content in the starting powder on the dielectric loss and the dissipation factor of LPS alumina ceramics.

In general, k' is higher in the present LPS materials that may possibly be due to the presence of impurities and added dopants. The tape cast $C2_S$i material also shows a higher *d.f.* and correspondingly higher loss (Table 3) compared to the same LPS materials fabricated by uniaxial pressing. Such a behavior can be attributed to the alignment of platelets during tape casting as revealed in the micrographs presented in our previous report [19].

3.5. Voltage dependence of dielectric constant, dissipation factor and dielectric loss

Fig. 5 shows the voltage dependence of k', *d.f.* and loss at power frequency i.e. 50 Hz, for $A6_M$ material. It is seen that the *d.f.* increases as the applied electrical

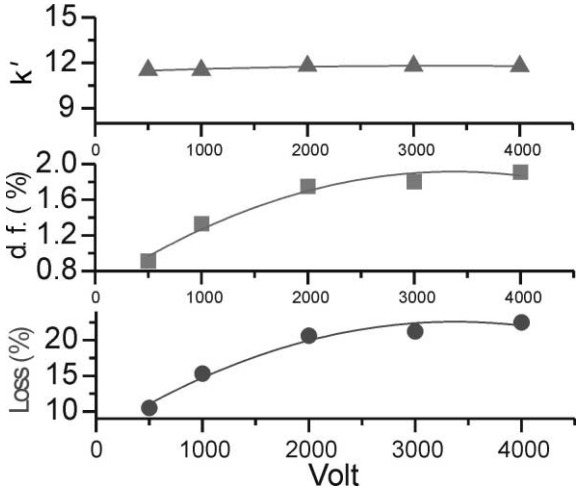

Fig. 5. Dielectric behavior at different voltage in a 91–94 wt.% LPS alumina ($A6_M$).

load increases and consequentially loss increases. The k' is hardly affected by the increase in the applied voltage whereas the *d.f.* and the resultant loss rise steadily up to 2 kV beyond which it remains unchanged.

4. Conclusion

The study showed that the alkalis and alkaline earth oxides present as impurities in the grain boundary glass influenced the dielectric properties of the LPS alumina ceramics. Because of impurities, the dielectric constant of the LPS materials was higher and the resistivity was lower compared to that of the pure alumina. Use of low Na_2O (non-reactive) alumina powder in the LPS ceramics resulted in lower dielectric loss at 1 MHz frequency. The dielectric properties did not show any improvement when reactive powder was used. The MgO/(CaO + BaO + KNaO) ratio in the chemical composition of the LPS was found to influence the dielectric loss but only in the lower frequency band (100–1000 Hz). At higher frequency, the difference was not significant. When the test voltage was increased from 500 V to 2000 V, the dissipation factor and the dielectric loss was found to be increased, and beyond 2000 V the effect was negligible. The study showed that both the coarse and the medium powders could be used in place of the costly reactive powders for superior dielectric properties in liquid-phase-sintered alumina ceramics.

Acknowledgements

The authors (A.P.G. and S.R.) are grateful to BHEL management for necessary support. The authors are also thankful to Professor A.M. Umarji, Indian Institute of Science for valuable discussions.

References

[1] R.H. Insley, Electrical properties of alumina ceramics, in: L.D. Hart (Ed.), Alumina Chemicals: Science and Technology Handbook, The American Ceramic Society, Westerville, OH, 1990, pp. 293–297.
[2] R. Morrell, Handbook of Properties of Technical and Engineering Ceramics, Part I, An Introduction for Engineers and Designers, National Physical Laboratory, Her Majesty's Stationary Office, London, 1985, pp. 162–167.
[3] A.E. Badger, J.F. White, Relation of electrical conductivity to chemical composition of glasses, J. Am. Ceram. Soc. 23 (1940) 271–274.
[4] F.A. Kroger, Electrical properties of α-Al_2O_3, in: W.D. Kingery (Ed.), Structure and Properties of MgO and Al_2O_3, Advances in Ceramics, Vol. 10, The American Ceramic Society Inc, Columbus, OH, 1984, pp. 1–15.
[5] J.L. Kemp, A.J. Moulson, The effect of iron addition on the electrical properties of alumina ceramics, Proc. Br. Ceram. Soc. 18 (1970) 53–64.
[6] J. Cohen, J. Am. Ceram. Soc. 44 (9) (1961) 459–464.
[7] W.D. Kingery, H.K. Bowen, D.R. Uhlmann, Introduction to Ceramics, 2nd Edition, John Wiley & Sons, New York, 1976, pp. 876–941 and 105.
[8] R.C. Buchanan, Properties of ceramic insulator, in: R.C. Buchanan (Ed.), Ceramic Materials for Electronics, Marcel Dekker, Inc, New York, 1986, pp. 1–77.
[9] W.D. Kingery, Grain boundary phenomena in electronic ceramics, in: L.M. Levinson (Ed.), Grain Boundary Phenomena in Electronic Ceramics, Advances in Ceramics Vol. 1, The American Ceramic Society, Inc, Columbus, OH, 1981, pp. 1–22.
[10] W.H. Gitzen (Ed.), Alumina as a Ceramic Material. The American Ceramic Society. Inc, Columbus, OH, 1970.
[11] J. Molla, R. Moneno, R. Vila, M. Gonzlez, A. Ibarra, Effect of impurities on alumina dielectric properties: magnesium, Bol Soc Esp. Ceram.Vidriro 36 (1) (1997) 21–24.
[12] M.D. Ingram, Mixed alkali effect revisited—a new look at an old problem, Glasketch Ber-Glass Sci. Tech. 67 (6) (1994) 151–155.
[13] A.J. Moulson, J.M. Herbert, Electroceramics, Chapman & Hall, London, 1992, pp. 182–263.
[14] W.O. Williamson, Particle orientation in clays and whitewares and its relation to forming process, in: W.D. Kingery (Ed.), Ceramic Fabrication Process, The Technology Press of MIT and John Wiley & Sons Inc, New York, 1958, pp. 89–98.
[15] S.J. Reed, Forming processes, part VII, in: Introduction to the Principles of Ceramic Processings, John Wiley & Sons Inc., New York, 1988, pp. 327–407.
[16] A.P. Goswami, S. Roy, M. Mitra, G.C. Das, Impurity-dependent morphology and grain growth in liquid-phase-sintered Al_2O_3, J. Am. Ceram. Soc. 84 (2001) 1620–1626.
[17] A.P. Goswami, S. Roy, M. Mitra, G.C. Das, Microstructure dependent hardness and fracture behavior in liquid-phase-sintered Al_2O_3, Ceram. Int. 26 (2000) 397–410.
[18] A.P. Goswami, S. Roy, M. Mitra, G.C. Das, Influence of powder, chemistry and microstructure on the wear resistance of liquid-phase-sintered Al_2O_3, Wear 244 (2000) 1–14 (and erratum 248 (2000) 227).
[19] A.P. Goswami, G.C. Das, Role of fabrication route and sintering on wear and mechanical properties of liquid-phase-sintered alumina, Ceram. Int. 26 (2000) 397–410.
[20] T.J. Carbone, in: L.D. Hart (Ed.), Alumina Chemicals: Science and Technology Handbook, The American Ceramic Society, Westerville, OH, 1990, pp. 99.
[21] D150-92 Annual Book of ASTM Standard, Philadephia, PA, p. 1187.